Computer-Assisted and Robot-Assisted Technologies to Improve Bone-Cutting Accuracy When Integrated with a Freehand Process Using an Oscillating Saw

Olivier Cartiaux, Laurent Paul, Pierre-Louis Docquier, Benoit Raucent, Etienne Dombre, Xavier Banse

Computer-Assisted and Robot-Assisted Technologies to Improve Bone-Cutting Accuracy When Integrated with a Freehand Process Using an Oscillating Saw

By Olivier Cartiaux, PhD, Laurent Paul, PhD, Pierre-Louis Docquier, MD, PhD, Benoît Raucent, PhD, Etienne Dombre, PhD, and Xavier Banse, MD, PhD

Investigation performed at the Centre for Research in Mechatronics and the Department of Orthopaedic Surgery, Université catholique de Louvain, Louvain-la-Neuve, Belgium

Background: In orthopaedic surgery, many interventions involve freehand bone cutting with an oscillating saw. Such freehand procedures can produce large cutting errors due to the complex hand-controlled positioning of the surgical tool. This study was performed to investigate the potential improvements in cutting accuracy when computer-assisted and robot-assisted technologies are applied to a freehand bone-cutting process when no jigs are available.

Methods: We designed an experiment based on a geometrical model of the cutting process with use of a simulated bone of rectangular geometry. The target planes were defined by three variables: a cut height (t) and two orientation angles (β and γ). A series of 156 cuts were performed by six operators employing three technologically different procedures: freehand, navigated freehand, and robot-assisted cutting. After cutting, we measured the error in the height t, the absolute error in the angles β and γ, the flatness, and the location of the cut plane with respect to the target plane.

Results: The location of the cut plane averaged 2.8 mm after use of the navigated freehand process compared with 5.2 mm after use of the freehand process ($p < 0.0001$). Further improvements were obtained with use of the robot-assisted process, which provided an average location of 1.7 mm ($p < 0.0001$).

Conclusions: Significant improvements in cutting accuracy can be achieved when a navigation system or an industrial robot is integrated into a freehand bone-cutting process when no jigs are available. The procedure for navigated hand-controlled positioning of the oscillating saw appears to be easy to learn and use.

Clinical Relevance: These findings support a recommendation for further study to determine if the improvements in cutting accuracy observed in vitro are possible in vivo.

In orthopaedic surgery, many interventions involving bone cutting with an oscillating saw require cutting accuracy. In most cases, a guidance apparatus is used during the cutting process to achieve the required accuracy. The most common example is knee arthroplasty, in which the obvious axes of the leg and the clear working space of the knee have facilitated the development and the integration of cutting jigs and slotted blocks in the bone-cutting procedure. However, several interventions still require purely freehand bone cutting because the anatomy, the bone geometry, and the working space available around the bone do not enable the use of jigs and/or cutting blocks. This is especially the case during pelvic bone-tumor resection in oncological surgery[1-3], periacetabular osteotomies in the treatment of acetabular dysplasia[4-7], pelvic osteotomies for hip reconstructive surgery in children[8-11], and talar osteotomy in total ankle arthroplasty[12,13].

In a study in which pelvic bone-tumor resection was simulated[14], the cutting accuracy with a conventional freehand

Disclosure: In support of their research for or preparation of this work, one or more of the authors received, in any one year, outside funding or grants in excess of $10,000 from Fonds National de la Recherche Scientifique (FNRS, Télévie, Belgium) (grant 7.4570.06) and Fondation Belge contre le Cancer (grant SCIE 2006/20). Neither they nor a member of their immediate families received payments or other benefits or a commitment or agreement to provide such benefits from a commercial entity.

technique (with no cutting jigs available) was demonstrated to be insufficient. The experiments were performed on simulated bones by experienced surgeons. The probability that a surgeon would achieve a 5-mm tolerance on the desired cutting plane under ideal working conditions was estimated to be 52%. The geometrical complexity and the restricted working space of the pelvic architecture aggravate the error arising from hand-controlled positioning of the surgical tool.

Computer-assisted and robot-assisted technologies have been developed to increase the geometrical accuracy of bone-cutting procedures involving the use of oscillating saws in conjunction with cutting jigs and guides, such as in knee arthroplasty[15]. Commercially available navigation systems may be used to guide some pin-fixed slotted blocks[15-18], and several robots are capable of controlling the positioning of these blocks around the osseous structure being cut[19-23]. The cuts are then performed manually by the surgeon inserting the saw blade into the prepositioned block.

Few attempts have been made to adapt these assistance technologies to freehand bone-cutting processes that do not involve conventional jigs and slotted blocks, such as osteotomies within the pelvis. Some studies have shown the feasibility of navigating a chisel[24-26], a burr[27], or some virtual screws[28,29] to perform and stabilize pelvic osteotomy sites. To our knowledge, only two studies[30,31] have shown the feasibility of directly navigating an oscillating saw to perform the bone cuts of total knee arthroplasties or to perform bone alignment osteotomies of the tibia. As far as we know, no one has compared the performance of a computer-assisted or a robot-assisted bone-cutting process with that of a purely freehand technique (without jigs) for using an oscillating saw.

We investigated the potential improvements in cutting accuracy resulting from the integration of computer-assisted and robot-assisted technologies into a freehand process of bone-cutting with an oscillating saw when no cutting jigs or slotted blocks are available. So that our results would be independent of the surgical application and any clinical aspect of a bone-cutting process, we designed an experimental test bed involving a simulated bone of simple geometry. We specifically addressed the following research question: Is the cutting accuracy improved when a navigation system or robot is integrated into a freehand bone-cutting process?

Materials and Methods

The tests were conducted with use of simulated bones made from solid rigid polyurethane closed foam (Sawbones/Pacific Research Laboratories, Vashon, Washington)[32]. The simulated bones consisted of blocks of rectangular geometry (size, $40 \times 40 \times 85$ mm) with a dimensional tolerance of 0.1 mm and a density of 0.84 g/cm^3 according to the manufacturer (Fig. 1). The clamping device consisted of two precision vises to fix the bone rigidly at each end. A pneumatic oscillating saw (Compact Air Drive II; Synthes, Solothurn, Switzerland) equipped with a 100-mm-long, 19-mm-wide, and 1.4-mm-thick blade (Synthes) was used to make all cuts in the central part of the simulated bones without jigs or slotted guides.

We designed a geometrical model of the cutting process to define the target planes (the desired planes after cutting) and to evaluate the accuracy of the cut planes (see Appendix). In summary, the target planes were defined by a minimal set of three independent variables: the height (t) measured in millimeters and two angles (depth, β, and front, γ) measured in degrees. We constructed three target planes with the following values for t, β, and γ, respectively: Plane 1 (25, 30, and 10), Plane 2 (30, 10, and –20), and Plane 3 (45, –20, and 20). To evaluate the accuracy of the cut planes (see Appendix), we defined two parameters, flatness (F) and location (L), measured in millimeters, in accordance with the ISO1101:2004 standard[33]. Previous experiments[34] have demonstrated the relevance of L in gathering all information about translational and rotational errors in the independent variables t, β, and γ.

We also designed three cutting processes (see Appendix for technical details): freehand cutting (Process 1), navigated freehand cutting (Process 2), and robot-assisted cutting (Process 3). For the freehand process, the operators cut the simulated bones without the use of jigs or guides. For the navigated freehand process, the operators were provided with visual feedback of the position and orientation of the saw blade with respect to the simulated bone. Finally, the robot-assisted process consisted of fully automated cutting.

A series of seventy-two cuts was performed with use of Process 1. Six operators (Operators 1 through 6) who were experienced in bone cutting each performed twelve cuts, four cuts in each of the three target planes, alternating among Plane 1, Plane 2, and Plane 3. Next, a series of seventy-two cuts was made with the aid of a navigation system (Surgetics; Praxim, Grenoble, France) (Process 2) by the same operators (Operators 1 through 6) using the same cutting sequence as employed for the freehand cutting process. The operators performed these cuts using the free mode of the navigation system with real-time visual feedback of the cut on a monitor screen. Finally, a series of twelve cuts was performed by an industrial six-axis robot (Viper s650; Adept Technology, Livermore, California) (Process 3) employing the same cutting sequence as used for the freehand and the navigated freehand cutting processes. An operator (Operator 1) used a handheld terminal to control normal starting and stopping procedures and emergency stops.

Statistical Analysis

We performed preliminary cuts with the freehand cutting process to calculate how many samples were required to have an 80% chance of detecting a difference at the 5% level of significance, as described by Petrie[35]. For these preliminary cuts, the location of the cut plane with respect to the target plane averaged approximately 5 mm. With an expectation of a 2 and 4-mm improvement in location with the navigated freehand and robot-assisted processes, respectively, a minimum of thirty-six samples was required for the navigated freehand process and a minimum of nine, for the robot-assisted process.

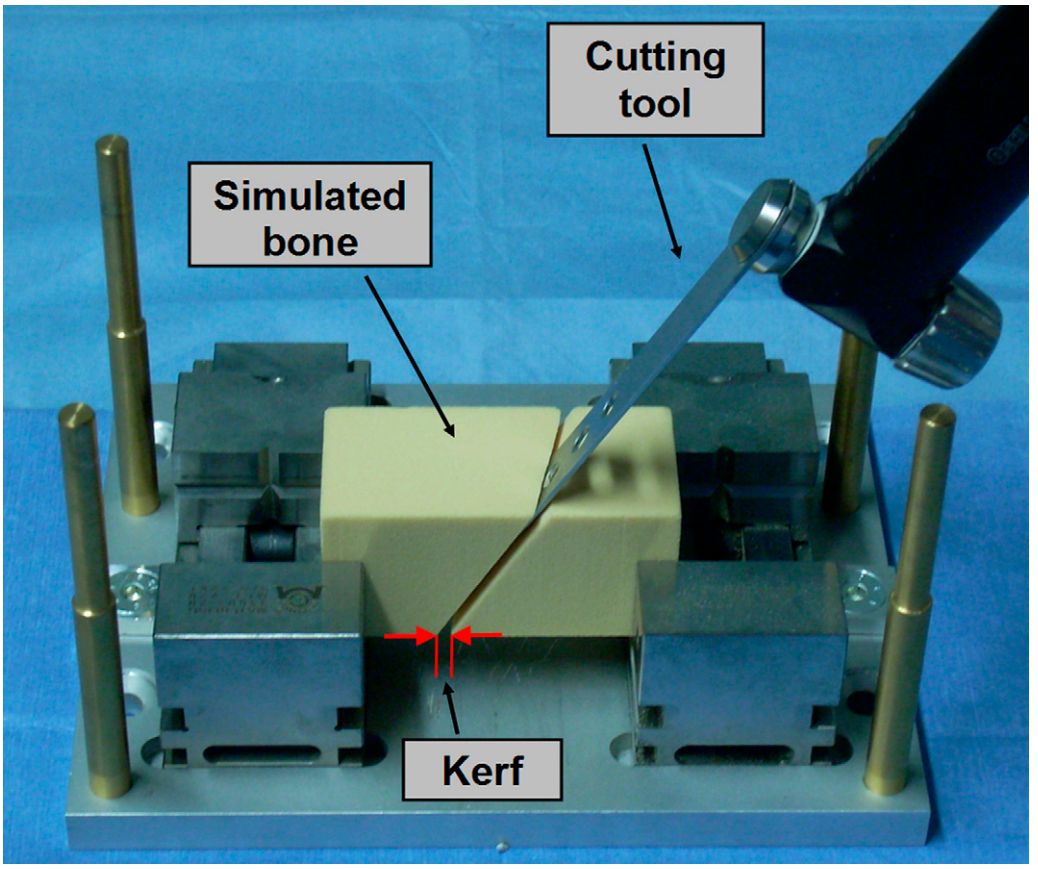

Fig. 1

Bone cutting performed with an oscillating saw when no jigs are available. The simulated bone is a polyurethane foam block simulating bone density and is clamped by means of two precision vises. The kerf is the loss of matter, which depends on the type of surgical cutting tools.

We performed an analysis of variance on repeated measurements, as described by Armstrong et al.[36]. The three cutting processes (Process 1: freehand, Process 2: navigated freehand, and Process 3: robot-assisted) were considered fixed effects, while the six operators (Operators 1 through 6) and the three target planes (Plane 1, Plane 2, and Plane 3) were considered random effects. Differences between mean values were determined with use of the Fisher test, and p values of <0.05 were considered significant. Results are presented as the mean and standard deviation.

We performed the statistical analyses of the rotational variables β and γ with use of the absolute values of the rotational errors. We did not analyze the signs of the rotational errors, and we thus considered a positive error and a negative error with the same absolute value to be equivalent from a statistical point of view.

Source of Funding

Grants from the Fonds National de la Recherche Scientifique (FNRS, Télévie, Belgium) (grant 7.4570.06) and Fondation Belge contre le Cancer (grant SCIE 2006/20) were used to pay for the salaries of laboratory personnel and for purchase of the bone models and surgical supplies.

Results

The error in the height of the cut plane was significantly decreased by the robot-assisted process (Fig. 2, *A*). The error was –0.92 ± 0.37 mm with the robot-assisted process compared with –1.26 ± 0.88 mm with the freehand process ($p < 0.0001$) and –1.87 ± 2.09 mm with the navigated freehand process ($p < 0.0001$).

Navigation assistance reduced the absolute error in the depth angle of the cut plane (1.79° ± 1.57°) (Fig. 2, *B*) relative to that associated with the freehand process (5.43° ± 4.39°; $p < 0.0001$). Navigation assistance produced a similar improvement in the absolute error in the front angle of the cut plane (1.46° ± 1.16°) relative to that associated with the freehand process (3.66° ± 3.16°; $p < 0.0001$). Further improvements were achieved with the robot-assisted process, with an average absolute error of 0.60° ± 0.46° for the depth angle and 0.73° ± 0.74° for the front angle ($p < 0.0001$ compared with the errors associated with the navigated freehand process). Finally, the absolute error in the front angle associated with the freehand process differed significantly from the absolute error in the depth angle associated with the freehand process ($p < 0.0001$). However, there was no significant difference between the depth and front angles in

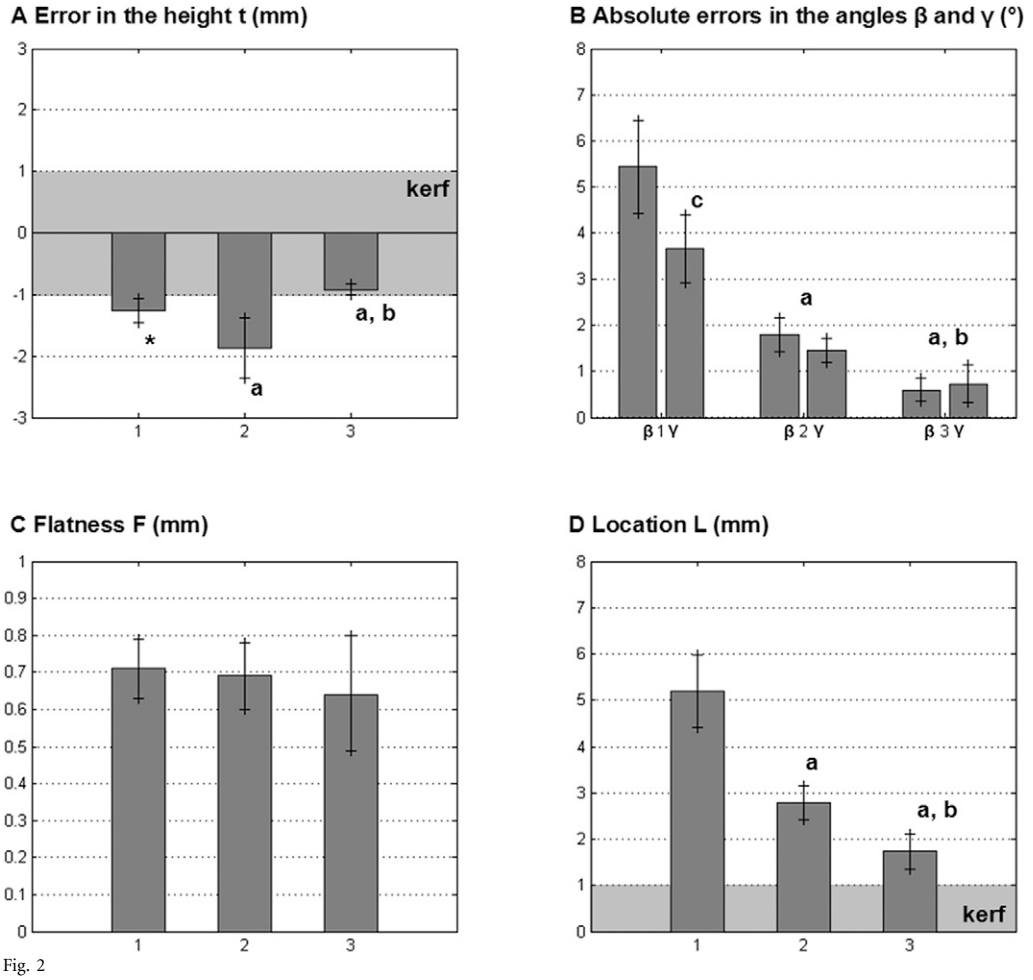

Fig. 2

Comparison of the error in the height (*t*), absolute errors in the depth and front angles (β and γ), flatness (*F*), and location (*L*) among the three cutting procedures: freehand (Process 1), navigated freehand (Process 2), and robot-assisted (Process 3). The kerf, defined in Figure 1, is illustrated in parts A and D. Mean values are shown with the lower and upper limits of the 95% confidence interval. *The entry point was marked with a pencil on the surface of the simulated bone. a = $p < 0.0001$ compared with Process 1; b = $p < 0.0001$ compared with Process 2; and c = $p < 0.0001$ for the difference between the errors in the depth and front angles for Process 1.

association with either the navigated freehand or the robot-assisted process.

The flatness of the cut plane did not vary significantly among the processes (Fig. 2, *C*). The flatness averaged 0.71 ± 0.34 mm after the freehand cutting, 0.69 ± 0.39 mm after the navigated freehand cutting, and 0.64 ± 0.27 mm after the robot-assisted cutting.

The location of the cut plane with respect to the target plane was significantly improved by the navigated freehand cutting process (Fig. 2, *D*). The location following use of the navigated freehand method averaged 2.78 ± 1.61 mm, compared with 5.19 ± 3.44 mm for that following use of the freehand cutting process ($p < 0.0001$). Further improvements were obtained with the robot-assisted cutting process, after which the average location was 1.73 ± 0.68 mm ($p < 0.0001$ compared with that associated with the navigated freehand process).

No significant differences were observed among the six operators or among the three target planes. Moreover, we did not observe any effect of a learning curve potentially induced by the cutting sequence.

Discussion

In this experimental study, we assessed the improvement in accuracy of bone cutting with an oscillating saw when computer-assisted and robot-assisted technologies were integrated into a surgical procedure with no available cutting jigs or guides. Because we wished our results to be independent of any surgical application, we designed a purely geometrical model of the cutting process involving a block of polyurethane foam that simulated a geometrically simple bone structure. The simulated bone was thus considered to be a uniformly solid material. This facilitated bone cutting with an oscillating saw with use of each of the three investigated processes. Additional

studies could be performed on more complex bone structures, simulated or real, that would present both trabecular and cortical layers.

Because this study dealt with the geometrical accuracy of bone cutting, we did not investigate clinical and functional parameters commonly discussed in the literature; these parameters include the fracture rate, nonunion rate, intraoperative time including the time to achieve the cuts, recovery time, flexion-extension or varus-valgus angles in total knee arthroplasty, safe margin during bone-tumor resection, alignment of the mechanical axis of the leg in a high tibial osteotomy, and forces applied during the cutting that could lead to thermal damage. Further research could be performed to incorporate these clinical, functional, and biological aspects into the cutting-process model.

To our knowledge, Barrera et al.[37] were the first to propose a purely geometrical methodology for evaluating cutting accuracy during total knee arthroplasties. They defined two global indices gathering all information about translational and rotational errors of the cut planes. Our methodology differed in that we used a unique and already standardized evaluation parameter (location) on a generalized model of the bone-cutting process. The location parameter provides the ability to gather all information about translational and rotational errors of a cut plane with respect to a target plane[34].

Belvedere et al.[38] showed the feasibility of assessing the accuracy of resection-plane alignment during total knee replacement. Using the sensor tool of a navigation system, the authors measured the femoral and tibial angles and the achieved mechanical axis. Both the location parameter and our methodology (measurement of e_t, e_β, and e_γ) could also be used intraoperatively to assess the accuracy of planar bone-cutting.

Our study demonstrated significant improvements in accuracy (as defined by location and flatness) when bone cutting was performed freehand with the aid of a navigation system as compared with when purely freehand cutting was done. To our knowledge, Haider et al.[30] were the first to report the results of a comparison of a navigated freehand process using an oscillating saw with the results of a conventional pin-guided process for total knee arthroplasty. They demonstrated that femoral implant alignment errors were smaller when the cutting had been performed with the aid of a navigation system. The location parameter data in our generalized model are consistent with those findings.

Further improvements in accuracy were observed when the bone cutting was performed by a robot. We believe that we are the first to evaluate a fully automated process for bone cutting with an oscillating saw. Burghart et al.[39] developed a semi-active cutting process for craniofacial operations in which an oscillating saw is manually guided along the cutting trajectory while a robot restricts the surgeon's movements. They demonstrated the feasibility of performing osteotomies with a deviation within 3 mm of the planned trajectory.

In our model, the flatness of the cut plane was not improved by the assistance of a navigation system or robot, reflecting the fact that all of the cuts were performed with use of only one kind of surgical cutting tool, the oscillating saw. Macdonald et al.[40] reported that significantly better flatness could be achieved if the oscillating saw were assisted by a purely mechanical system. However, they based their evaluation methodology on the flatness defined by Toksvig-Larsen and Ryd[41] as the standard deviation of the measured points. The flatness defined by Toksvig-Larsen and Ryd is not the same as the flatness defined in the ISO1101:2004 standard[33] that we used in this study. The flatness, if defined as the measurement standard deviation, is closer to the microscopic notion of roughness as defined in the ISO1101:2004 standard. We did not investigate such microscopic properties of the cut plane.

The error in the cut-plane height was subject to significant variation. The error associated with the robot-assisted process was significantly decreased compared with that associated with the purely freehand and navigated freehand processes. However, the error associated with the navigated cutting was larger than that associated with the freehand process. Accounting for both kerf (loss of matter, which depends on the oscillating saw) during the tool calibration step and correcting for blade flexure during the cuts (for example, by measuring the forces applied to the blade) are two potential solutions for decreasing the global translational error.

Siston et al.[15] reviewed the controversy surrounding the use of surgical navigation for total knee arthroplasty. There is some debate regarding whether the sagittal and coronal alignments of the tibial component are improved by the use of a navigation system[16]. The angles β and γ used to define the target planes in our cutting model can be seen as flexion/extension and varus/valgus alignment specifications for a tibial cut. With the significantly decreased errors of the angles β and γ, our data support the idea that a navigation system improves cutting in both the sagittal and the coronal plane. Moreover, all of the operators reported that they felt confident performing the navigated freehand bone cutting with an oscillating saw. The real-time visual feedback was found to be sufficiently accurate and meaningful. The navigation system provided useful three-dimensional information so that there was no significant difference between the absolute error in the depth angle of the cut plane and the absolute error in the front angle of the cut plane, in contrast to the significant difference between these errors observed with the freehand technique.

Fadda et al.[42] argued that using an oscillating saw in conjunction with a robot arm would be impossible because of the reaction forces exerted on the saw blade at the beginning of the cut. Our study demonstrates the feasibility of using a robot as a tool-holder in a cutting process involving a conventional oscillating saw. The robot-assisted process provided the best performance in terms of cutting accuracy when compared with either the navigated freehand or the purely freehand cutting

process. However, we concur with Fadda et al. that currently employed oscillating saws may not be the most suitable tools for robot-assisted technology because of their limited capability to produce surfaces without gaps. The study by Fadda et al. demonstrated that a milling device held by a robot manipulator can handle a 0.2-mm maximum gap for the cut surface. This is about three times smaller than the order of flatness obtained during our experiment with an oscillating saw.

Appendix

eA Descriptions of the freehand, navigated freehand, and robot-assisted cutting processes and figures depicting the definition of the quality of the cut planes as well as the cutting processes are available with the electronic version of this article on our web site at jbjs.org (go to the article citation and click on "Supporting Data"). ■

Olivier Cartiaux, PhD
Benoît Raucent, PhD
Centre for Research in Mechatronics,
Université catholique de Louvain,
Place du Levant 2, B-1348 Louvain-la-Neuve,
Belgium.
E-mail address for O. Cartiaux: olivier.cartiaux@uclouvain.be

Laurent Paul, PhD
Pierre-Louis Docquier, MD, PhD
Xavier Banse, MD, PhD
Department of Orthopaedic Surgery,
Université catholique de Louvain,
Avenue Mounier 53, 1200 Bruxelles,
Belgium

Etienne Dombre, PhD
LIRMM, CNRS-Université Montpellier 2,
161 rue Ada, 34392 Montpellier CEDEX 05,
France

References

1. Delloye C, Banse X, Brichard B, Docquier PL, Cornu O. Pelvic reconstruction with a structural pelvic allograft after resection of a malignant bone tumor. J Bone Joint Surg Am. 2007;89:579-87.

2. Donati D, El Ghoneimy A, Bertoni F, Di Bella C, Mercuri M. Surgical treatment and outcome of conventional pelvic chondrosarcoma. J Bone Joint Surg Br. 2005; 87:1527-30.

3. Hoffmann C, Gosheger G, Gebert C, Jürgens H, Winkelmann W. Functional results and quality of life after treatment of pelvic sarcomas involving the acetabulum. J Bone Joint Surg Am. 2006;88:575-82.

4. Clohisy JC, Barrett SE, Gordon JE, Delgado ED, Schoenecker PL. Periacetabular osteotomy in the treatment of severe acetabular dysplasia. Surgical technique. J Bone Joint Surg Am. 2006;88 Suppl 1(Pt 1):65-83.

5. Ito H, Matsuno T, Minami A. Chiari pelvic osteotomy for advanced osteoarthritis in patients with hip dysplasia. J Bone Joint Surg Am. 2004;86:1439-45.

6. Siebenrock KA, Leunig M, Ganz R. Periacetabular osteotomy: the Bernese experience. J Bone Joint Surg Am. 2001;83:449-55.

7. Schramm M, Hohmann D, Radespiel-Troger M, Pitto RP. The Wagner spherical osteotomy of the acetabulum. Surgical technique. J Bone Joint Surg Am. 2004;86 Suppl 1:73–80.

8. Turgeon TR, Phillips W, Kantor SR, Santore RF. The role of acetabular and femoral osteotomies in reconstructive surgery of the hip: 2005 and beyond. Clin Orthop Relat Res. 2005;441:188-99.

9. Wedge JH, Thomas SR, Salter RB. Outcome at forty-five years after open reduction and innominate osteotomy for late-presenting developmental dislocation of the hip. Surgical technique. J Bone Joint Surg Am. 2008;90 Suppl 2(Pt 2):238-53.

10. Grudziak JS, Ward WT. Dega osteotomy for the treatment of congenital dysplasia of the hip. J Bone Joint Surg Am. 2001;83:845-54.

11. López-Carreño E, Carillo H, Gutiérrez M. Dega versus Salter osteotomy for the treatment of developmental dysplasia of the hip. J Pediatr Orthop B. 2008;17: 213-21.

12. Clare MP, Lee WE 3rd, Sanders RW. Intermediate to long-term results of a treatment protocol for calcaneal fracture malunions. J Bone Joint Surg Am. 2005;87:963-73.

13. Rammelt S, Zwipp H. Calcaneus fractures: facts, controversies and recent developments. Injury. 2004;35:443-61.

14. Cartiaux O, Docquier PL, Paul L, Francq BG, Cornu OH, Delloye C, Raucent B, Dehez B, Banse X. Surgical inaccuracy of tumor resection and reconstruction within the pelvis: an experimental study. Acta Orthop. 2008;79:695-702.

15. Siston RA, Giori NJ, Goodman SB, Delp SL. Surgical navigation for total knee arthroplasty: a perspective. J Biomech. 2007;40:728-35.

16. Kim YH, Kim JS, Choi Y, Kwon OR. Computer-assisted surgical navigation does not improve the alignment and orientation of the components in total knee arthroplasty. J Bone Joint Surg Am. 2009;91:14-9.

17. Dutton AQ, Yeo SJ, Yang KY, Lo NN, Chia KU, Chong HC. Computer-assisted minimally invasive total knee arthroplasty compared with standard total knee arthroplasty. A prospective, randomized study. J Bone Joint Surg Am. 2008;90:2-9.

18. Biant LC, Yeoh K, Walker PM, Bruce WJ, Walsh WR. The accuracy of bone resections made during computer navigated total knee replacement. Do we resect what the computer plans we resect? Knee. 2008;15:238-41.

19. Pott PP, Scharf HP, Schwarz ML. Today's state of the art in surgical robotics. Comput Aided Surg. 2005;10:101-32.

20. Taylor RH, Stoianovici D. Medical robotics in computer-integrated surgery. IEEE Trans Rob Autom. 2003;19:765-81.

21. Maillet P, Nahum B, Blondel L, Poignet P, Dombre E. BRIGIT, a robotized tool guide for orthopedic surgery. In: Proceedings of the 2005 IEEE International Conference on Robotics and Automation (ICRA); 2005 Apr 18-22. Barcelona, Spain: IEEE Publications; 2005. p 211-6.

22. Plaskos C, Cinquin P, Lavallée S, Hodgson AJ. Praxiteles: a miniature bone-mounted robot for minimal access total knee arthroplasty. Int J Med Robot. 2005;1:67-79.

23. Ritschl P, Machacek F, Fuiko R. Modern navigated ligament balancing in total knee arthroplasty with the PiGalileo system. In: Stiehl JB, Konermann WH, Haaker RG, DiGioia AM 3rd, editors. Navigation and MIS in orthopedic surgery. Heidelberg: Springer Medizin; 2007. p 135-40.

24. Hüfner T, Kfuri M Jr, Galanski M, Bastian L, Loss M, Pohlemann T, Krettek C. New indications for computer-assisted surgery: tumor resection in the pelvis. Clin Orthop Relat Res. 2004;426:219-25.

25. Krettek C, Geerling J, Bastian L, Citak M, Rücker F, Kendoff D, Hüfner T. Computer aided tumor resection in the pelvis. Injury. 2004;35 Suppl 1:S-A79-83.

26. Langlotz F, Bächler R, Berlemann U, Nolte LP, Ganz R. Computer assistance for pelvic osteotomies. Clin Orthop Relat Res. 1998;354:92-102.

27. Cho HS, Kang HG, Kim HS, Han I. Computer-assisted sacral tumor resection. A case report. J Bone Joint Surg Am. 2008;90:1561-6.

28. Wong KC, Kumta SM, Chiu KH, Antonio GE, Unwin P, Leung KS. Precision tumour resection and reconstruction using image-guided computer navigation. J Bone Joint Surg Br. 2007;89:943-7.

29. Mayman DJ, Rudan J, Yach J, Ellis R. The Kingston periacetabular osteotomy utilizing computer enhancement: a new technique. Comput Aided Surg. 2002;7:179-86.

30. Haider H, Barrera OA, Garvin KL. Minimally invasive total knee arthroplasty surgery through navigated freehand bone cutting. J Arthroplasty. 2007;22:535-42.

31. Weber S, Lueth TC. Navigation of bone alignment osteotomies of the tibia. Int J Med Robot. 2005;1:98-107.

32. ASTM International. Standard F1839-08e1: Standard specification for rigid polyurethane foam for use as a standard material for testing orthopedic devices and instruments. West Conshohocken, PA: ASTM International; 2008.

33. International Organization for Standardization. Standard 1101:2004: Geometrical Product Specifications (GPS)—geometrical tolerancing—tolerances of form,

orientation, location and run-out. 2nd ed. Geneva, Switzerland: International Organization for Standardization; 2004.

34. Cartiaux O, Paul L, Docquier PL, Francq BG, Raucent B, Dombre E, Banse X. Accuracy in planar cutting of bones: an ISO-based evaluation. Int J Med Robot. 2009;5:77-84.

35. Petrie A. Statistics in orthopaedic papers. J Bone Joint Surg Br. 2006;88:1121-36.

36. Armstrong RA, Eperjesi F, Gilmartin B. The application of analysis of variance (ANOVA) to different experimental designs in optometry. Ophthalmic Physiol Opt. 2002;22:248-56.

37. Barrera OA, Haider H, Garvin KL. Towards a standard in assessment of bone cutting for total knee replacement. Proc Inst Mech Eng H. 2008;222:63-74.

38. Belvedere C, Ensini A, Leardini A, Bianchi L, Catani F, Giannini S. Alignment of resection planes in total knee replacement obtained with the conventional technique, as assessed by a modern computer-based navigation system. Int J Med Robot. 2007;3:117-24.

39. Burghart C, Krempien R, Redlich T, Pernozzoli A, Grabowski H, Muenchenberg J, Albers J, Hassfeld S, Vahl C, Rembold U, Woern H. Robot assisted craniofacial surgery: first clinical evaluation. In: Computer Assisted Radiology and Surgery. Proceedings of the 13th International Congress and Exhibition; 1999 Jun 23-26; Paris, France. New York: Elsevier; 1999. p 828-33.

40. Macdonald W, Styf J, Carlsson LV, Jacobsson CM. Improved tibial cutting accuracy in knee arthroplasty. Med Eng Phys. 2004;26:807-12.

41. Toksvig-Larsen S, Ryd L. Surface flatness after bone cutting. A cadaver study of tibial condyles. Acta Orthop Scand. 1991;62:15-8.

42. Fadda M, Marcacci M, Toksvig-Larsen S, Wang T, Meneghello R. Improving accuracy of bone resections using tool holder and a high speed milling cutting tool. J Med Eng Technol. 1998;22:280-4.

43. Anselmetti B. Tolérancement: cotation de fabrication et métrologie. Vol 3. Paris: Lavoisier; 2003.

44. Clohisy JC, Barrett SE, Gordon JE, Delgado ED, Schoenecker PL. Periacetabular osteotomy in the treatment of severe acetabular dysplasia. Surgical technique. J Bone Joint Surg Am. 2006;88 Suppl 1(Pt 1):65-83.

45. Khalil W, Dombre E. Modélisation identification et commande des robots. 2nd ed. Paris: Hermes Science Publications; 1999.

Appendix E-1

Geometrical Model of the Cutting Process

The target planes (the desired planes after cutting) were defined by a minimal set of three independent variables (t, β, and γ) in a geometrical reference frame (R_0) with a reference plane (A) (Fig. E-1). The variable t represents the height of the target plane measured in millimeters along the Z axis of R_0. The variable β represents the depth angle measured in degrees in the YZ plane of R_0. The variable γ represents the front angle measured in degrees in the XZ plane of R_0 that corresponds to the front face of the simulated bones during the cuts. To obtain a large range of depth and front angles, we constructed three target planes with the following values for t, β, and γ, respectively: Plane 1 (25, 30, and 10), Plane 2 (30, 10, and −20), and Plane 3 (45, −20, and 20). Plane 1 and Plane 2 have positive depth angles while Plane 3 has a negative depth angle. Practically, the operators had to position their wrist in substantial ulnar deviation to perform the cuts of Plane 3.

To evaluate the cutting error, we defined two parameters, flatness (F) and location (L), in accordance with the ISO1101:2004 standard[33]. F represents the form of the cut plane and is defined as the minimum distance in millimeters between two parallel planes that include the cut plane (Fig. E-2). L refers to the position of the cut plane with respect to the target plane (Fig. E-2). L is defined as half the distance in millimeters between two planes that present the following properties: they are parallel to the target plane, they are positioned at an equal distance from the target plane, and they include the cut plane. Previous experiments[34] have demonstrated the relevance of L in gathering all information about translational and rotational errors in the independent variables t, β, and γ.

Evaluation of the Cutting Process

To evaluate the cutting errors, we first digitized the cut planes with a precision of 1 μm using a coordinate measuring machine (SIGNUM SL; Mycrona, Elgin, Illinois) with a spherical sensor (2 mm in diameter). The cut-plane digitization was performed according to the guidelines for an ISO-based evaluation of macroscopic properties such as location and flatness[43]: the 2-mm diameter of the spherical sensor enabled us to neglect microscopic properties such as roughness. The initial cut-plane data set consisted of a matrix of 10 × 10 measurement points, consisting of a squared distribution on the cut section of the simulated bone and acquired in the z-direction of R_0 with the zero reference considered to be the reference plane A (Fig. E-2). We then fitted this coordinate set to a least square plane, a common procedure in checking ISO parameters[43].

The cutting errors were calculated with use of numerical computation software (MATLAB; The MathWorks, Natick, Massachusetts). The error e_t was calculated as the distance along the Z axis of R_0 between the least square plane and the target plane. The error e_β was calculated as the angular difference in the YZ plane of R_0 between the normals of the least square plane and the target plane. The error e_γ was calculated as the angular difference in the XZ plane of R_0 between the normals of the least square plane and the target plane. Because the three target planes covered a large range of depth and

front angles, we also calculated the rotational errors in terms of their absolute values ($e_{|\beta|}$, $e_{|\gamma|}$).

To determine the parameter *F,* we calculated the maximum and minimum distances (f_{max} and f_{min}), normal to the least square plane, between the measured points and the least square plane; *F* was then calculated as the sum of the absolute values of f_{max} and f_{min}. The parameter *L* was calculated as the absolute value of the maximum distance, normal to the target plane, between the measured points and the target plane.

Process 1: Freehand Cutting

A series of seventy-two cuts was performed with use of the freehand cutting process. Six operators (Operators 1 through 6), experienced in bone cutting, each performed twelve cuts, four cuts in each of the three target planes, alternating among Plane 1, Plane 2, and Plane 3. For the freehand process, the operators cut the simulated bones without the use of jigs and guides. We allowed the operators to palpate the simulated bones before the cuts to introduce them to the bone anatomy. We then covered the surgical site with a blue drape that had holes to simulate realistic conditions (Fig. E-3) (for example, in periacetabular surgery[9,44] and ankle surgery[12]). Our goal was to limit the (lateral) visibility and accessibility to the bone and also to prevent the operators from defining geometrical landmarks on the precision vises or the rectangular geometry of the simulated bones (which would have been an unrealistic and irrelevant action). To provide an estimate of the depth and front angles, a printed sheet with a graduated angular scale from 0° to 30° in 5° increments was given to the operators. Finally, the entry point of the target planes was marked with a pencil on the surface of the simulated bone starting from reference plane A, while the exit point was hidden by the blue drape.

Process 2: Navigated Freehand Cutting

A series of seventy-two cuts was performed with the aid of a navigation system (Surgetics; Praxim, Grenoble, France) by the same operators (Operators 1 through 6) using the same cutting sequence as employed in Process 1. A computed tomography scan (made with a spiral Elscint Twin CT Medical Scanner [ElsMed, Holon, Israel]) of the simulated bone was made with 0.4-mm x-y resolution and a 1.1-mm slice thickness with a 0.7-mm step in the z-direction. The navigation system can handle slice thicknesses of 1 to 3 mm. We constructed a three-dimensional model of the simulated bone by using reconstruction and segmentation algorithms provided by the navigation system. To minimize the modeling error of the simulated bone, we constructed the three target planes by defining the independent variables (t, β, and γ) starting from reference plane A (the bottom face of the polyurethane block, corresponding to the bottom face of the three-dimensional model), as described in Figure E-1.

The navigated freehand process was designed to provide operators with visual feedback of the position and orientation of the saw blade with respect to the simulated bone (Fig. E-4). The navigation system employed the spine module that enables the planning and navigation of intrapedicular screw insertions. We adapted this module for direct navigation of the saw blade around the simulated bone. The main geometrical dimensions of the blade were included in the system, and the oscillation plane of the blade was calibrated with use of the calibration unit. Finally, we registered the simulated bone with the three-dimensional computed tomography model using paired-point and

surface-based algorithms provided by the navigation system. This registration step was performed only once before the navigated cuts were performed, since our experimental test bed allowed us to fix the simulated bones at exactly the same position. After registration, we checked its accuracy by sensoring a set of ten points on each face of the simulated bone. We calculated the distances between these points and the three-dimensional bone model with the measuring tool of the navigation system. These distances were always smaller than 0.5 mm; this is within the accuracy of the localizer (Polaris; NDI, Waterloo, Ontario, Canada), which has an accuracy of 0.5 mm and 0.5° according to the manufacturer.

A dynamic reference basis was rigidly fixed to the bone-clamping device. The dynamic reference basis and the oscillating saw were equipped with patterns of infrared reflecting markers. The Polaris localizer tracked these patterns with an accuracy of 0.5 mm and 0.5°. Using the tracking information, we were able to calculate the position and orientation of the saw blade with respect to the reference frame R_0 attached to the simulated bone. The operators performed the cuts using the free mode of the navigation system with real-time visual feedback of the cut on a monitor screen.

Process 3: Robot-Assisted Cutting

A series of twelve cuts was performed with use of an industrial six-axis robot (Viper s650; Adept Technology, Livermore, California). According to the manufacturer, the robot has an XYZ positioning repeatability of ±0.03 mm. The internal calibration of the robot (originally performed by the manufacturer) was verified, as described by Khalil and Dombre[45]. Geometrically simple motions of the end-effector, such as linear and circular segments, were defined into the work volume of the application and programmed into the robot controller. An external optical localizer (MicronTracker Hx40; Claron Technology, Toronto, Ontario, Canada) tracked the position and the orientation of the end-effector equipped with a black-and-white marker, with an accuracy of 0.5 mm and 0.5°. We then verified that the robot performed the desired motions within the accuracy of the localizer.

The robotic process was designed for fully automated cutting. The robot and the bone-clamping device were mounted on the same worktable. The oscillating saw was rigidly attached to the wrist of the robot (Fig. E-5). The MicronTracker localizer was used to sensor both the faces of the simulated bone and the end-effector of the robot by using a tracking pointer marked with a black-and-white pattern.

Starting from the points of the simulated bone sensored by the MicronTracker localizer, we constructed the bone model and the reference frame R_0, as described in Figure E-1, by fitting the faces XY (reference plane A), YZ, and XZ of the simulated bone to a least square plane. We then constructed the target planes by defining the three independent variables (t, β, and γ) starting from the reference plane A. After that, we checked the accuracy of the registration between the simulated bone and the bone modeled in the robot controller by sensoring a set of ten points on each face of the simulated bone. We calculated the distances between these points and the three-dimensional bone model. These distances were always smaller than 0.5 mm; this is also within the accuracy of the MicronTracker localizer.

Finally, starting from the points sensored on the end-effector of the robot and knowing the kinematic parameters of the robot, we calculated the position of the robot

base with respect to the simulated bone and calibrated the position and orientation of the saw blade in the reference frame R_0.

We programmed the robot controller with a cutting-process algorithm to move the oscillating saw blade along the target planes. To bypass the absolute positioning error of an industrial six-axis robot (typically induced by gravity, and of an order of magnitude of a few millimeters), we developed our cutting-process algorithm to control the robot motions relative to the initial calibrated position of the saw blade in the reference frame R_0, as described by Khalil and Dombre[45]. An operator (Operator 1) used a handheld terminal to control normal starting and stopping procedures and emergency stops. The robot translation speed was set at 10 mm/s.

Appendix E-2

Discussion About the Error in the Cut-Plane Height

The error in the cut-plane height was subject to significant variations (Fig. 2, *A*). With the robot-assisted process, the error was significantly decreased compared with that associated with the purely freehand and navigated freehand processes. However, the error associated with the navigated cutting was larger than that observed with the freehand process. We can discuss these results by presenting three major considerations:

1. Cutting bones with an oscillating saw with a 1.4-mm-thick blade produced a kerf of an order of 2 mm (Fig. 1). The kerf was measured on the twelve cuts of the robot-assisted process. We did not account for this kerf during the evaluation of the cutting processes. Therefore, we can reasonably expect a negative bias equal to half a kerf (about 1 mm) on the calculated errors of the cut-plane height and location (Fig. 2, *A* and *D*). By definition, this kerf has no influence on the rotational errors or the flatness (Fig. 2, *B* and *C*). As a consequence, accounting for the kerf in the discussion, the translational error encountered when positioning the oscillating saw was about 0.1 mm for the robot, 0.9 mm for the operators assisted by the navigation system, and 0.3 mm for the operators working freehand.

2. Cutting bones with an oscillating saw with a 100-mm-long blade produced some flexure of the blade. We did not account for this deformation in the navigation system. We visually noted a flexure of the blade induced by the operator, just before the cutting, when he placed the saw in contact with the simulated bone to position the blade according to the visual feedback provided by the system. The flexure was not present in the robot-assisted process because the robot motions were programmed into the controller, and it was not present in the freehand process because the entry point of the target plane was marked on the surface of the simulated bone.

3. We favored the freehand cutting process by marking the entry point of the target plane on the surface of the simulated bone, while the exit point was hidden by the blue drape with holes. Marking the entry point with a pencil on the bone surface simulated a surgical reality: before performing freehand bone-cutting, surgeons can use a marker to place some landmarks on the skin in order to guide the cutting[12,14]. In our study design, we decided to mark the entry point beforehand in order to prevent the operators from defining landmarks on the precision vises or the simple rectangular bone geometry, which would have been an unrealistic and irrelevant action. For the robot-assisted process, the entry point was automatically virtually defined in the robot controller by

defining the independent variables (t, β, and γ) in the constructed reference frame R_0. For the navigated freehand process, the entry point had to be reached by positioning the oscillating saw on the bone surface according to the visual feedback provided by the system. However, even if the freehand cutting process was favored, the results first revealed a relatively small 0.9-mm error for the navigated positioning of the saw (Fig. 2, *A*) and secondly demonstrated that location was nevertheless significantly improved by the navigation system (Fig. 2, *D*).

As a conclusion about the cut-plane height, we think that both accounting for kerf during the tool calibration step and correcting for blade flexure during the cuts (for example, by measuring the forces applied to the blade) are two potential solutions for improving the global translational error.

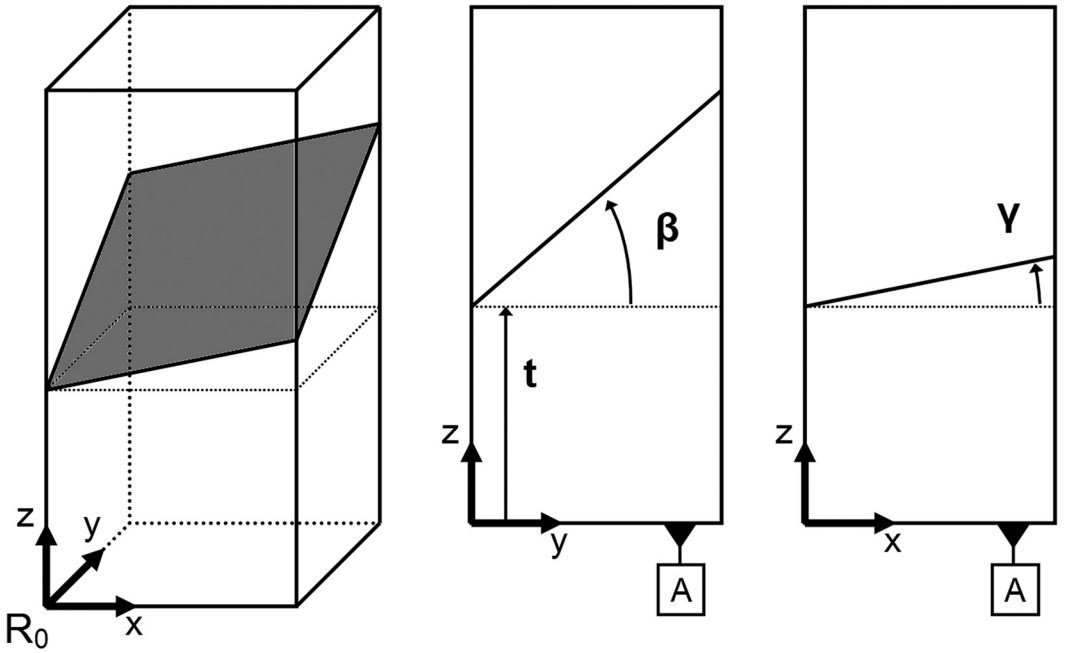

Fig. E-1
Geometrical model of the cutting process. The target plane (the gray plane in the three-dimensional view) is defined in a reference frame R_0 by a set of three independent variables: height (t) in millimeters, depth angle (β) in degrees, and front angle (γ) in degrees. A = the reference plane for the definition of t, β, and γ.

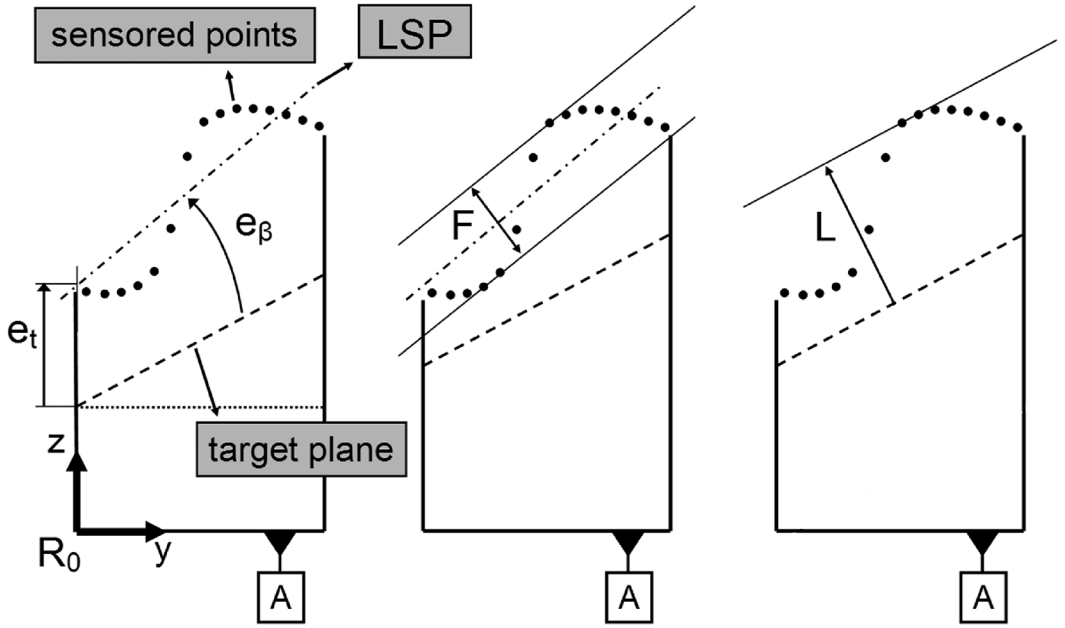

Fig. E-2
Definition of the cutting errors: error in the height (e_t) in millimeters, error in the depth angle (e_β) in degrees, flatness (F) in millimeters, and location (L) in millimeters. The target plane is the dashed line. The cut plane is sampled by the measurement points (the sensored points). The measurement points are fit to a least square plane (LSP). A (the bottom face of the block in the left panel) = the reference plane for the definition of t, β, and γ.

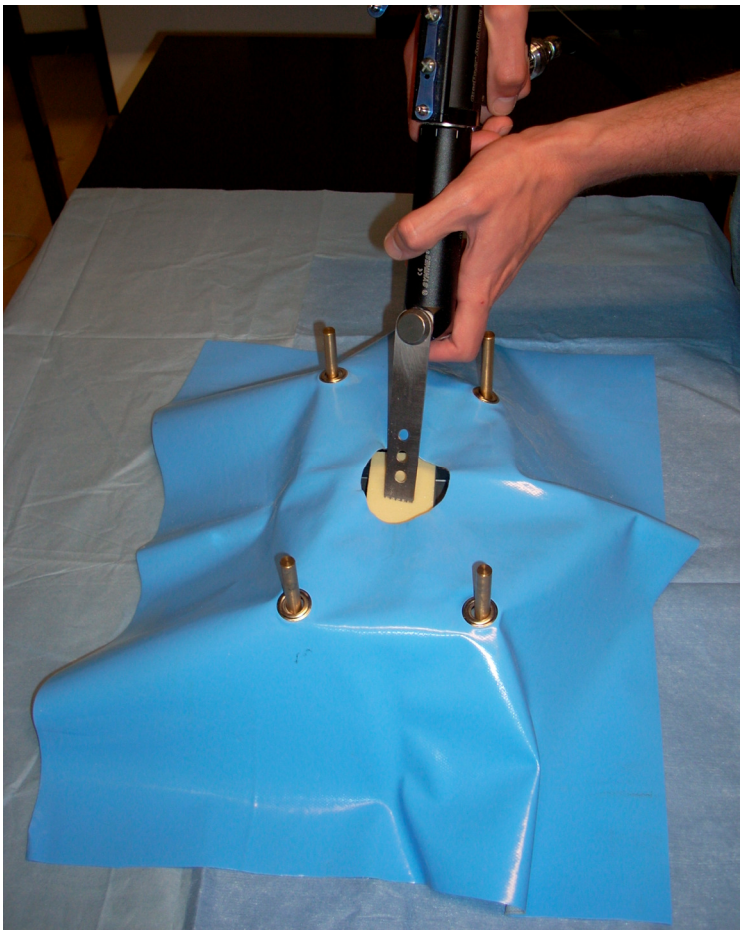

Fig. E-3
The freehand cutting process with no available jigs. A blue drape with holes covered the simulated bone to prevent the operators from defining geometrical landmarks on the precision vises or the rectangular geometry of the simulated bones.

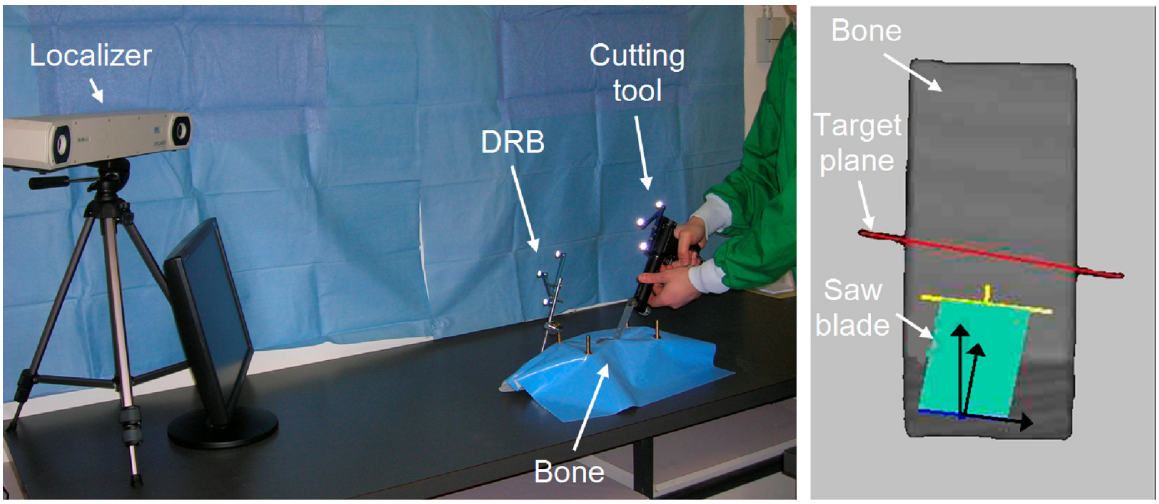

(a) (b)

Fig. E-4
a: The navigated freehand cutting process with no available jigs. A dynamic reference basis (DRB) is fixed to the simulated bone. The oscillating saw is tracked in real time by an optical localizer. *b:* The real-time visual feedback consists of a virtual three-dimensional model of the simulated bone. The target plane is represented by a red line. The position and orientation of the saw blade are continuously refreshed. The oscillation plane of the blade is represented by a green rectangle delimited by a yellow line (the distal extremity of the blade) and a blue line (the proximal extremity of the blade). The blade is correctly aligned on the target plane when the red, yellow, and blue lines overlap.

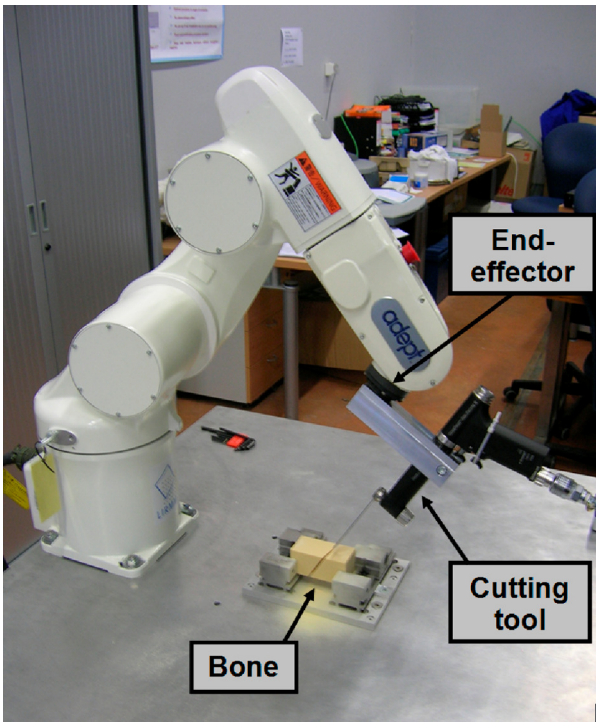

Fig. E-5
The robot-assisted cutting process. The oscillating saw is rigidly attached to the end-effector of the robot. The simulated bone and the saw blade were previously registered and calibrated by using an external optical localizer. The robot controlled the position and orientation of the saw blade in the reference frame R_0 (defined in Fig. E-1).